CHEMISTRY
A EUROPEAN JOURNAL

DOI: 10.1002/chem.200700922

Star-Shaped Oligobenzoates: Non-conventional Mesogens Forming Columnar Helical Mesophases

Matthias Lehmann,*[a] Michael Jahr,[a] Bertrand Donnio,[b] Robert Graf,[c] Sibylle Gemming,[d] and Igor Popov[d]

Abstract: Star-shaped mesogens with a phloroglucinol or a trimesic acid core and oligobenzoate arms with up to five repeating units have been synthesised. These non-conventional mesogens form various columnar mesophases over a broad temperature range. The liquid-crystal phases were characterised by optical microscopy, differential scanning calorimetry, X-ray diffraction, dilatometry and solid-state NMR spectroscopy. In addition to the high-temperature hexagonal columnar phases, the columnar self-assemblies undulate upon cooling and consequently form higher-ordered body-centred orthorhombic columnar 3D structures. A model of *E*-shaped folded conformers helically displaced along the columns is proposed. Helical preorganisation in the hexagonal phase precedes the transition to the low-temperature phases. Space filling and nano-segregation compete in the self-organisation process, thus aliphatic chains and the polar oligobenzoate scaffold are not perfectly separated in these star-shaped mesogens.

Keywords: liquid crystals · oligobenzoates · solid-state NMR spectroscopy · star-shaped mesogens · X-ray diffraction

Introduction

In the last decade, increasing numbers of non-conventional liquid crystals have been synthesised.[1] Among the different structures are multiarm-mesogens, dendrons, dendrimers,[2–4] and supramolecular mesogens, such as metallomesogens[5] and hydrogen-bonded mesogens.[6] If adequately designed, these compounds can be used as soft functional materials, for example, anisotropic electron/hole-, ion-, proton-conducting and opto-electronic materials. Nano-segregation of chemically and/or physically different molecular segments has been shown to play a key role in self-assembly of mesogens in liquid-crystal (LC) structures,[7–9] as previously observed with lyotropic systems and block copolymers. One family of non-conventional mesogens are star-shaped molecules with three arms. Many examples are known that have various three-armed cores as well as different numbers and positions of flexible aliphatic chains.[10–18] Molecules with no lateral chains[17b] or internal short alkoxy chains[11c] form nematic phases, whereas mesogens with more than six long peripheral aliphatic chains frequently assemble into columnar structures.[10a,b,g,11a,b,d–g,12a,c,d,13–16,17c,f,18] With only three aliphatic chains on the periphery, a broad range of phases can be found: crystalline phases as well as nematic, smectic and columnar mesophases. Evidently, flexibility of the core is an important parameter with respect to supramolecular self-assembly. Oligobenzoates can be characterised as semi-flexible molecules (Figure 1). The individual oxyphenylcarboxy groups are flat and shape-persistent; however, the single C–O bonds to the ester oxygen atoms allow the formation of a large number of different star-, *E*- and *T*-shaped conformers.[19] If most extended star-shaped conformers are drawn schematically with C_3 symmetry, as shown in Figure 1, there is an unoccupied volume between the arms. In crystal structures of star-shaped molecules with propyloxy chains, the

[a] Dr. M. Lehmann, M. Jahr
Institute of Chemistry, Chemnitz University of Technology
Straße der Nationen 62, 09111 Chemnitz (Germany)
Fax: (+49) 371-531-1839
E-mail: matthias.lehmann@chemie.tu-chemnitz.de

[b] Dr. B. Donnio
Institut de Physique et Chimie des Matériaux de Strasbourg - IPCMS, UMR 7504 - CNRS/Université Louis Pasteur
23, rue Loess, BP 43, 67034 Strasbourg Cedex 2 (France)

[c] Dr. R. Graf
Max-Planck-Institut of Polymer Research
Ackermannweg 10, 55128 Mainz (Germany)

[d] Dr. S. Gemming, I. Popov
Institute of Physical Chemistry and Electrochemistry
Dresden University of Technology
Mommsenstraße 13, 01062 Dresden (Germany)

Supporting information for this article is available on the WWW under http://www.chemeurj.org/ or from the author.

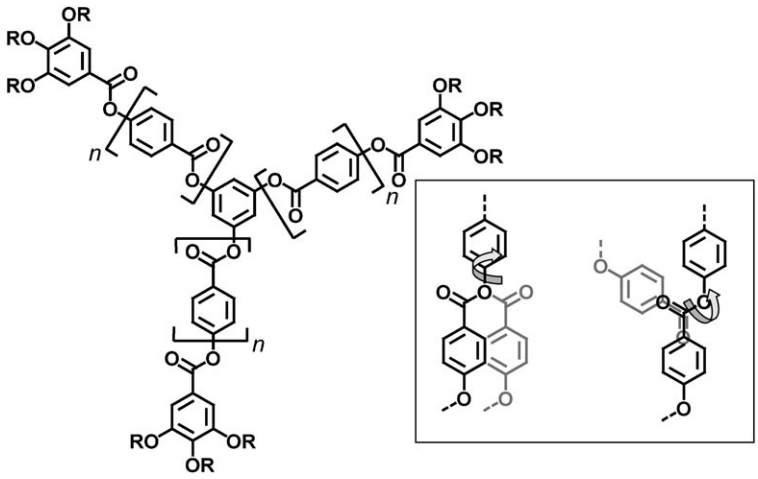

Figure 1. Star-shaped oligobenzoates. Semi-flexibility is illustrated by the rotation about the C–O single bonds.

void can be filled by solvent or by neighbouring molecules, or even by mixing the different molecular segments.[20,21] Such compensation is not possible in the neat liquid crystal. Assuming nano-segregation and coplanar stacking of these extended molecules, thus with only one molecule in the unit cell, the model structure would possess an unreasonably low density.[21] Consequently, self-assembly in which disk-shaped molecules stack on top of each other, as observed with discotic mesogens in hexagonal mesophases,[22] is unlikely. A series of C_3-symmetric oligobenzoates has been prepared to study the packing behaviour of star-shaped mesogens.[18a] The increasing size of the oligobenzoate arms also increases the void within these structures in the C_3-symmetric, star-shaped compounds. Nevertheless, all of the molecules in the series have been found to form columnar mesophases: a high-temperature hexagonal columnar phase (Col_h) and a low-temperature columnar mesophase. Column diameters were very small compared with the diameters of the star-shaped conformers[18a] and shape-persistent mesogens of comparable structure and size.[11e,f] Thus, other derivatives were proposed, such as *E*-shaped conformers, which explain the X-ray results. Evidence for *E*-shaped conformers was obtained from the discovery of a helical crystal phase formed from the monotropic hexagonal mesophase upon annealing at ambient temperature.[23] Helical mesophases were recently found for similar compounds, for example within a series of stilbenoid derivatives,[11a,b] cyclotriphosphazenes[15a,b] and wedge-shaped molecules.[3] In this contribution, we explore the different mesophases, which includes the previously described helical crystal phase, by X-ray scattering on oriented fibres (wide-angle X-ray scattering (WAXS) and small-angle X-ray scattering (SAXS)), dilatometry studies and solid-state NMR spectroscopy. We demonstrate that the low-temperature phases of star-shaped semi-flexible oligobenzoates generally consist of columns with a 3D organisation, which is based on undulated structures best described by helically packed *E*-shaped mesogens. There is evidence that a partial helical assembly in the hexagonal phase precedes the transition to the highly ordered mesophases. Star-shaped compounds with different cores have also been synthesised (Figure 2 and Scheme 1) to study the steric and electronic effects of the structural changes on the conformer and thus on self-assembly in the columnar mesophase.

Results and Discussion

Synthesis: The synthesis of the various star-shaped derivatives is shown in Scheme 1. Star-shaped mesogens **1** were prepared as previously described.[18a] Triiodo derivatives **2** were obtained analogously by using triiodophloroglucinol[24] as the core. Compound **3** was synthesised by threefold esterification of 1,3,5-benzenetricarbonyl trichloride (trimesic acid trichloride) with 4-(3,4,5-tridodecyloxybenzoyloxy)phenol. The latter compound is an arm derivative that was prepared from a mono-benzyl-protected hydroquinone and 3,4,5-tridodecyloxybenzoic acid. All of the compounds were successively purified and analysed by using standard methods (see the Experimental Section). The materials were freeze-dried prior to their thermal study to prevent a rapid transesterification reaction at high temperatures.[25]

Molecular models—different conformations and the influence of different cores: Star-shaped mesogens consist of a highly flexible periphery, the alkyl chains, and a polar semi-flexible oligobenzoate interior. Previous investigations indicate that nano-segregation of these two different segments leads to LC columnar assemblies.[18] However, the column diameters were shown to be relatively small compared with the diameters of all-*s-trans* conformers (Figure 2, conformer A). Conformational analysis suggests that a folded conformer may play a role in the aggregation process.[19] Different conformations for the molecules can be obtained by rotation about the single bonds of the benzoate scaffold. There are three types of σ bonds 1) C–O bonds that connect aromatic rings with the carboxy groups, 2) C–C bonds that join the carboxy groups to the aromatic carbon atoms and 3) internal C–O bonds of the carboxy groups. Only rotation around the third type of σ bonds leads to a significant change in the molecular shape and size. Minimisation of the conformational energy of a single molecule of **1a** results in an almost planar structure with an all-*s-trans* conformation.[19] Only the middle benzoate groups are turned out of the plane and give rise to a dipole moment perpendicular to this plane. Such a conformation has recently been found for a star-shaped molecule in its single crystal obtained from acetone.[21] The crystal structure is stabilised by antiparallel

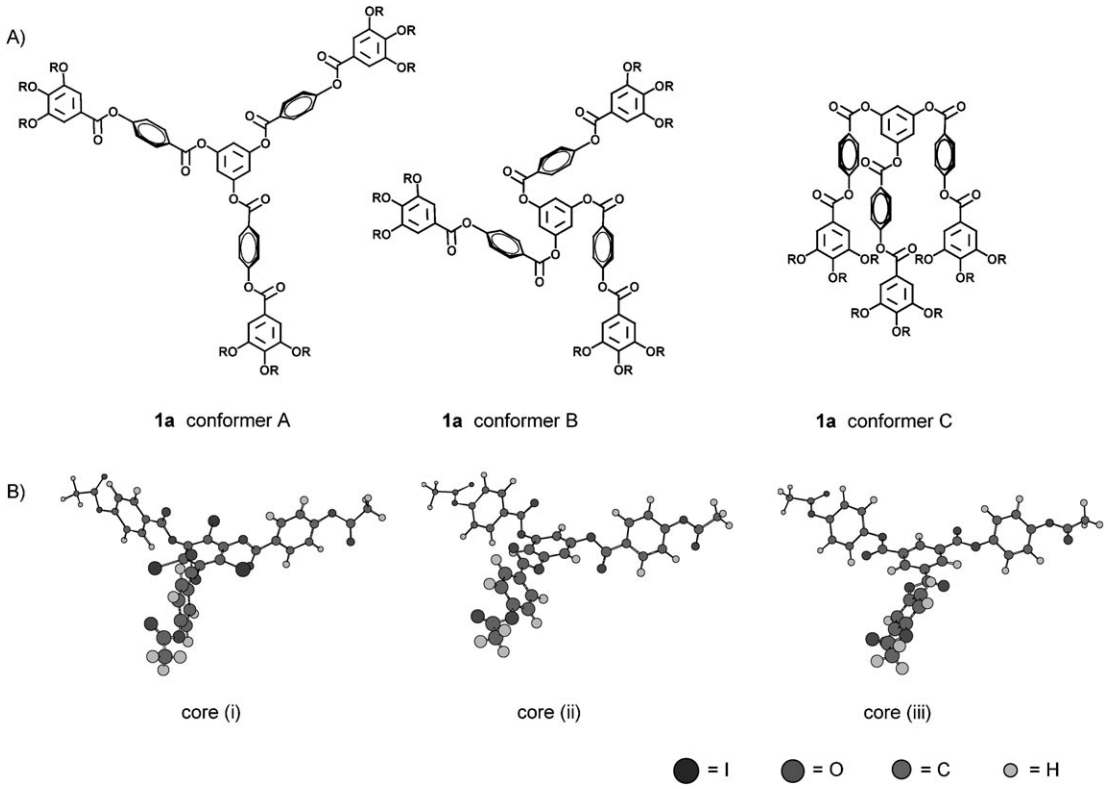

Figure 2. A) Different possible conformers of compound **1a**: star-shaped conformer A, folded star-shaped conformer B and *E*-shaped conformer C. B) Energy-minimised core structures (AM1). Core (i) is based on triiodophloroglucinol, core (ii) on phloroglucinol and core (iii) on trimesic acid.

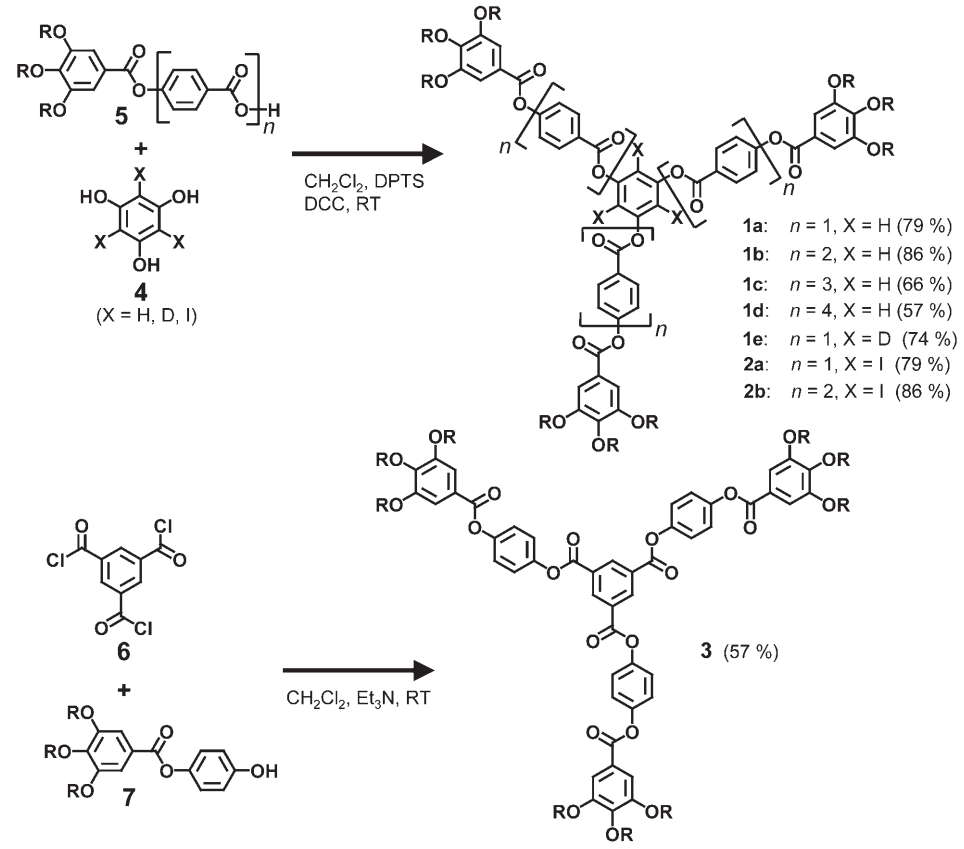

Scheme 1. Synthesis of star-shaped mesogens ($R = C_{12}H_{25}$).

aligned dipoles, and the benzoate arms interdigitate completely. However, such a conformer does not correctly explain the small column diameter measured. The change in shape and size is realised by rotation about the single bond of the carboxy group and is shown by conformers B and C (Figure 2), which might be possible structures; however, no proof has been obtained so far. Therefore, we synthesised iodine derivatives **2** and trimesic acid derivative **3**, which should show strong steric and electronic effects on the conformers B and C and, consequently, on the LC properties. Figure 2B visualizes the results on energy-minimised structures by the semi-empirical AM1 method. Iodine at the centre of the molecule introduces steric congestion, therefore, the middle benzoate units turn out of the plane by 90° relative to the central aromatic unit. Thus, core (i) pos-

sesses larger local dipoles perpendicular to the molecular plane than the core (ii), without iodine. If the inner carboxy group is inverted, that is, trimesic acid is used as central building block, the planar part of core (iii) is enlarged by the three carboxy groups, which are conjugated with the aromatic ring. The middle benzene rings of the benzoate arms can then freely rotate without producing a local dipole. Whereas the larger, planar core should stabilise the mesophases, the reduced dipole along the column could show the opposite effect.

Thermotropic properties: All of the materials were investigated by means of differential scanning calorimetry (DSC) and polarised optical microscopy (POM). Table 1 summarises the results of star compounds **1** to **3**. The data for the group of molecules with only one repeat building block between the central benzene ring and the peripheral gallic acid unit is shown in the first three entries. Inverting the inner carboxy group leads to a stabilisation of the columnar mesophase by 35 °C. This can be rationalised by a larger planar core for the latter compound (Figure 2). Consequently, iodo substitution, which causes the centre to be non-planar, should destabilise the liquid-crystal phase. Surprisingly, introduction of three iodo atoms at the phloroglucinol centre again results in the formation of a columnar mesophase, which is still stabilised by 3 °C compared to parent molecule **1a**. Similarly, larger molecule **2b** assembles in a columnar mesophase; however, the clearing temperature is lower than that of parent molecule **1b**. In contrast with mesogens **1a**, **1b** and **3**, which transform to mesophases of higher order at low temperature, the iodine derivatives always remain in hexagonal columnar phases. Mesogens **1a** and **3** also stay in the hexagonal phase when stored below the glass transition temperature as a LC glass. However, annealing for several days above the glass transition temperature converts the mesophases to phases of higher order with a waxy consistency that are characterised as soft crystalline materials. The hexagonal columnar mesophase of **1a** is thus monotropic. Enantiotropic Col_h phases are found for compound **3** and the extended mesogens **1b–d**. The temperature interval for the Col_h phases varies with the length of the oligobenzoate arms from 19 °C (**1b**), 9 °C (**1d**) to 2 °C (**1c**). At lower temperatures, higher-ordered body-centred orthorhombic mesophases are formed.

Table 1. DSC data of star-shaped mesogens.[a]

Compound	Onset phase transition temperatures [°C] (transition enthalpies [kJ mol^{-1}])				
1a	g	20	Col_h	53 (5.5)	I
	I	48 (6.0)	Col_h	20	g
	Cr_{borh}[b]	55 (32.7)	I		
2a	Col_h	58 (6.9)	I		
	I	50 (5.0)	Col_h[d]		
3	g	34	Col_h	89 (4.9)	I
	I	88 (4.5)	Col_h		
	Cr_{borh}[b]	74 (31.2)	Col_h	88 (4.8)	I[c]
1b	Col_{borh}	79 (11.6)	Col_h	98 (3.0)	I
	I	95 (2.8)	Col_h	70 (7.8)	Col_{borh}
2b	Col_h	82 (3.4)	I		
	I	78 (2.5)	Col_h		
1c	Col_{borh}	170 (10.1)	Col_h	172 (5.4)	I
	I	170 (4.2)	Col_h	166 (9.6)	Col_{borh}
1d	Col_{borh}	241 (11.4)	Col_h	251 (7.5)	I
	I	247 (4.8)	Col_h	234 (8.2)	Col_{borh}

[a] Col_h: high-temperature hexagonal phase, Col_{borh}: low-temperature orthorhombic body-centred phase, Cr_{borh}: soft crystal. [b] Annealing at room temperature leads to the formation of a soft crystal. [c] After several weeks at room temperature, compound **3** forms an additional non-shearable phase that transforms at 49 °C to the soft crystal. [d] Heating rate 2 °C min^{-1}.

POM investigations of compounds **1a–c**, **2b** and **3** show pseudo-focal-conic textures typically observed for columnar phases.[26] Figure 3 presents exemplary textures of materials **1a** and **1b**. Compound **2a** exhibits a mosaic texture, which is also frequently reported for hexagonal columnar mesophases (see the Supporting Information),[26c] whereas mesogen **1d** does not facilitate the formation of a characteristic texture owing to its thermal instability above 200 °C. The textures of **1b** and **1c** become more birefringent at the transition to the higher-ordered phases (Figure 3D, E). Interestingly, a completely dark image occurs during the transition between the low-temperature phase and the hexagonal mesophase of **1b**, which indicates a high degree of disorder in the reorganisation process. However, the almost identical textures in the high- and the low-temperature phases point to a close relationship between the two phases; for example, for the transformation of **1a** from the hexagonal columnar liquid-crystal phase to the soft crystal it was shown that the columnar structure remains.[23c] Despite the close relationship between the coarse structures, a fine pattern appears on the pseudo-focal-conic texture at low temperatures (Figure 3B and E); in the areas of the dark brushes it is similar to features found for undulated phases.[26a,27] The structureless, smeary texture obtained by shearing of the crystalline phase of **1a** demonstrates its softness (Figure 3C).

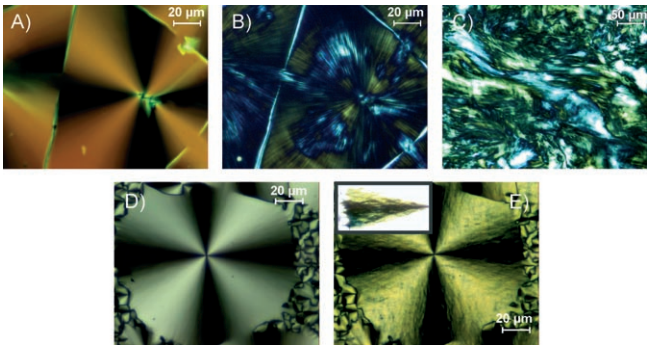

Figure 3. Textures of compounds **1a** and **1b**. A) Pseudo-focal-conic texture of **1a** in the Col_h phase at RT. B) Columnar Cr_{borh} phase of **1a** after 20 h at RT. C) Cr_{borh} of **1a** after shearing. D) Pseudo-focal-conic texture of **1b** in the Col_h phase at 92 °C. E) Texture at 74 °C in the Col_{borh} phase of **1b**. The inset shows the left dark brush at increased camera sensitivity.[28]

X-ray diffraction

Hexagonal phases: X-ray diffraction studies were performed on powder samples and/or on oriented fibres obtained by extrusion from the high-temperature LC phases.[29] The series **1a–d** has been recently investigated by powder X-ray diffraction by using a synchrotron source.[18] Herein, the hexagonal phases of **1c** and **1d** have not been investigated further because at these high temperatures transesterification reactions irreversibly damage the LC self-assembly during prolonged heating. Figure 4A and B show the WAXS patterns of extruded fibres of **1a** and **1b** in their high-temperature columnar LC phases. Intense reflections at the equator are related to columnar 2D order. Integration of the WAXS and SAXS patterns along the equator clearly shows a ratio of $1:\sqrt{3}:2$ for the reciprocal Bragg distances, which is evidence for hexagonal packing of the columns (Figure 4D). At wide angles, a diffuse halo is attributed to liquid-like aliphatic chains. For **1a**, the intensity on the halo is highest at the meridian, which points to an average orthogonal orientation of the mesogen cores with respect to the columnar axis. In contrast, the set of four maxima for **1b** on the halo indicates that the molecules are tilted by an average of 35°. Interestingly, for both materials a very diffuse X-ray intensity at small angles was observed on the meridian of the pattern. This may be attributed to some periodicity along the columns. Similar results were obtained with the high-temperature phase of **3** at 80 °C or with a freshly extruded sample at room temperature (see the Supporting Information).

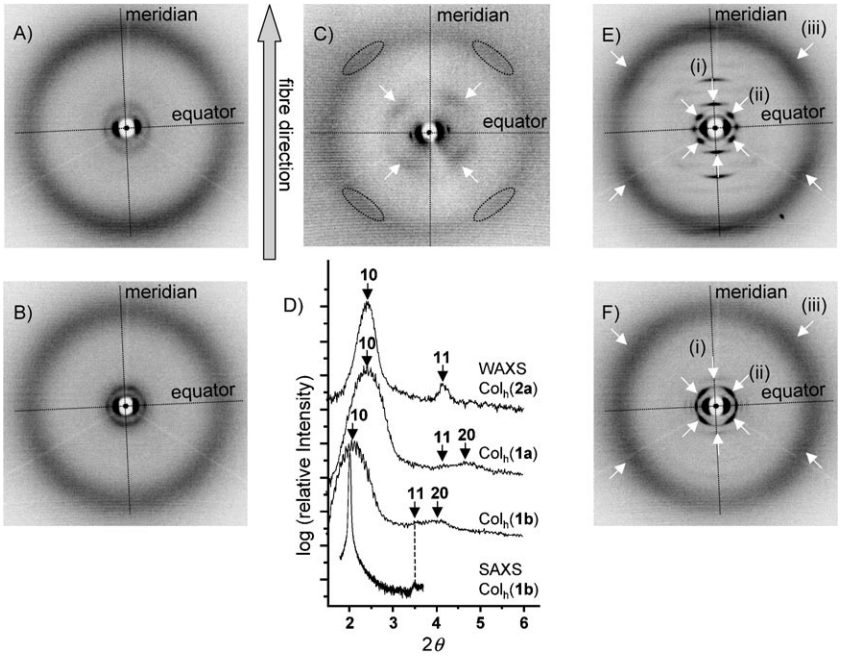

Figure 4. WAXS and SAXS pattern of extruded fibres of **1a**, **1b** and **2a**. A) Compound **1a** freshly extruded at 30 °C. B) Compound **1b** at 92 °C (2nd heating cycle). C) Compound **2a** at 30 °C. D) Integration along the equator of the patterns in A) to C); $1/d_{10}:1/d_{11}:1/d_{20}=1:\sqrt{3}:2$, which indicates a hexagonal structure. The 11 and 20 reflections of **1a** and **1b** are very broad with low intensity in WAXS, the SAXS of **1b** shows clearly the 11 reflections. E) Compound **1a** annealed for four days at ambient temperature. F) Compound **1b** at 60 °C after cooling from the hexagonal phase (B); i) 002 reflection, ii) set of four 211 reflections, iii) set of four reflections attributed to tilted mesogens.

X-ray diffraction of fibres of iodo derivatives **2a** and **2b** in their single mesophase show typical patterns for columnar phases, which consist of a halo at wide angles and reflections at the equator (Figure 4C). The corresponding reciprocal distances of the latter are related by $1:\sqrt{3}$ and thus substantiate a hexagonal 2D-structure (Figure 4D). A set of four diffuse reflections on the halo of the X-ray pattern is indicative for mesogens tilted with respect to the columnar axis. The set of four diffuse reflections at small angles points to additional order along the columns, which will be discussed later. Table 2 summarises the diameters of the columns in the hexagonal phases. The values increase with the size of the mesogens. Although, the different steric and electronic influences in derivatives **1a**, **2a**, **3**, **1b** and **2b**, respectively, could lead to different conformers in the LC phases and consequently to different column diameters, the latter values are almost matching for all molecules with the same number of repeating units.

Body-centred orthorhombic mesophases (Col_{borh}): Figure 4E and F show the WAXS patterns of material **1a**, annealed for four days at ambient temperature, and **1b** at 60 °C in the cooling scan. For all other derivatives **1c**, **1d**, and **3**, similar patterns were recorded in their low-temperature phases (see the Supporting Information).

Table 2. Cell parameter *a* of hexagonal columnar phases.

Compound	n[a]	T [°C]	a (Col_h) [Å][b]
1a	1	40	42.6
2a	1	30	42.6
3	(1)	80	42.1; 43.4[c]
1b	2	91	49.9
2b	2	70	50.6
1c	3	171	57.4[d]
1d	4	247	65[b]

[a] n = Number of benzoate repeating units (Figure 1); the number in parenthesis for compound **3** indicates the different hydroquinone repeating unit (Scheme 1). [b] Values obtained from SAXS investigations. [c] This value was obtained at RT in the supercooled Col_h phase of **3** from WAXS measurements. [d] Parameters from ref. [18].

As for the hexagonal phase, reflections at the equator reveal the maintained orientation of the material. Indeed, recent AFM studies of **1a** demonstrated that the transformation from the hexagonal phase into the low-temperature phase proceeds along the liquid-crystal columns that act as templates.[23c] Therefore, the equatorial reflections are attributed to 2D packing of columns and can be indexed according to a centred rectangular unit cell (see the Supporting Information). The halo at approximately 4.4 Å is characteristic for the liquid-like aliphatic chains. In contrast to the Col_h phases, in the rectangular phases many reflections are observed on layer lines along the meridian. These reflections indicate the correlation of the mesogens along the columns. The number of signals is larger for the small mesogens. However, the diffraction patterns of all materials have common meridional reflections (i), a set of four very intense reflections (ii) and a second set of four diffuse reflections at the halo (iii), as shown in Figure 4. The reflections indicated by (iii) may be related to inclined molecules within the columns. The other reflections, (i) and (ii), can be indexed as 002 and 211; of which the only exception is compound **3**, in which reflections (ii) correspond to the (011) planes. Reflections with Miller indices $h+k+l\neq 2n$ are not detected. Therefore the 3D assembly can be described as body-centred orthorhombic unit cells (Col_{borh}). Because the columnar organisation remains during the transition from the hexagonal to the orthorhombic phase, and also the reverse, 3D organisation into the orthorhombic cell may be achieved by undulation of columns.[30] Undulation correlates the neighbouring columns, although the aliphatic chains separating the polar cores (nano-segregation) are still liquid-like. Figure 5 illustrates a possible model.

Mixed indices $h,k,l\neq 0$ often indicate an underlying crystalline phase. The present materials are waxy and highly viscous; however, they are still shearable. The reflections are broad and correlation lengths calculated by the Scheerer formula[31] are thus relatively low (10–20 periods). Moreover, solid-state NMR experiments provide evidence for the mobility of molecular segments. Therefore, we assign the phases of **1a** and **3** to soft columnar crystals that are only obtained after prolonged annealing. In contrast, for the low-temperature phases of **1b–d**, which show reversible transitions with low hysteresis in cooling and heating cycles, we refer to undulated columnar liquid crystals. The cell parameters are summarised in Table 3. Parameters $a/2$ for **1a**, and b for all of the other compounds, compare well with the diameter of the corresponding hexagonal unit cells (Table 2), thus showing their relationship to the hexagonal columnar liquid crystals.

Table 3. Orthorhombic unit cells of low-temperature phases.

Mesogen	T [°C]	Unit cell parameter (Col_{borh}) [Å]			$d_{meridian}$ [Å] ($\xi d_{meridian}^{-1}$)[d]		d_{halo} [Å] (ξd_{halo}^{-1}; α [°])[d,e]	
		a	b	c	d_{002}	d_{211}[b]	Set of signals on the halo	Halo[f]
1a	31	77.2	35.6	34.0	17.0 (21)	20.8 (11)	4.4 (10; 60°)	4.4 (9)
3	30	64.3	47.0	64.6	32.7 (9)	37.8 (8)[c]	3.8 (11)[a], 4.4 (21)	4.4 (6)
1b	60	69.7	50.5	30.4	15.2 (20)	30.6 (10)	4.4 (20;58°)	4.5 (6)
1c	150	82.1	60.0	37.0	18.5 (17)	37.9 (8)	4.7 (6; 62°)	4.6 (6)
1d	190	93.3	68.6	43.0	21.5 (9)	41.9 (7)	4.7 (6; 66°)	4.8 (6)

[a] Diffuse signals at the meridian. [b] First set of split reflections at small angles. [c] d_{011}. [d] ξ Correlation length calculated by the Scheerer formula; the value of ξ/d in parenthesis provides an estimate for the number of correlated repeating units. [e] α is the angle between the diffraction vector and the column direction and corresponds to the inclination of the mesogens. [f] Halo attributed to the liquid-like chains.

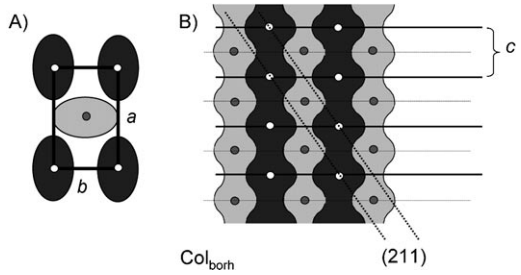

Figure 5. A) Section through a unit cell of the Col_{borh} phase orthogonal to the columnar axis. The elliptic cross-section of columns symbolises the inclined mesogens. B) Correlation of columns along direction c by undulation. The light grey columns are shifted by $a/2$ behind the plane of the drawing.

Solid-state NMR spectroscopy: ^1H and ^2H solid-state NMR spectroscopy studies have been performed on mesogen **1e**, which is a derivative of **1a** deuterated at the central phloroglucinol ring. To identify the conformation and the packing of the aromatic mesogens, ^1H double-quantum (DQ) NMR correlation spectra[32] have been recorded at $T=270$ and 300 K in the soft crystal phase. Because the 2D DQ spectra did not show any temperature dependence other than a significant line narrowing at higher temperature that resulted from increased molecular mobility and led to a better spectral resolution of the different proton sites, only the spectrum recorded at $T=300$ K is given in Figure 6.

The aliphatic, OCH_2 and the aromatic protons are well resolved, and all spatial proximities due to the chemical structure were confirmed (grey, horizontal lines in Figure 6a). The signal intensity of the aromatic signals and that of the OCH_2-protons is significantly enhanced by the DQ filtration compared to the aliphatic chains, as can easily be seen from Figure 6b. This indicates a lower molecular mobility of these moieties in contrast to the highly mobile aliphatic chains. The fact that the OCH_2 signal is even more pronounced than the aromatic signal arises from the closer spatial proximity (0.18 nm) of the two protons in this group compared with the closest proton–proton distance in a phenyl ring (0.24 nm) and cannot be directly attributed to a difference in molecular mobility.

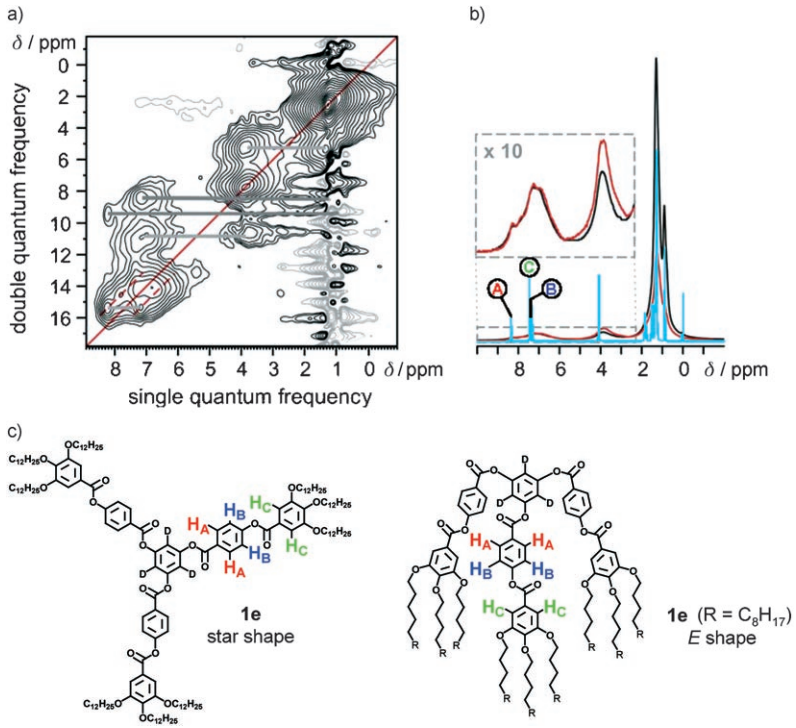

Figure 6. a) ^{1}H DQ correlation spectrum recorded at $T=300$ K sample temperature and 30 kHz MAS using 1 rotor period back-to-back (BaBa)[33] for DQ excitation. b) Comparison of signal intensities in ^{1}H DQ-filtered (——, 1 tR BaBa, 30 kHz MAS) and ^{1}H MAS NMR spectrum (——), normalised to the signal intensity of the aromatic protons. The solution ^{1}H NMR spectrum of **1e** (——) was recorded in $CDCl_3$ (400 MHz).

Most informative with respect to molecular conformations and the packing of the oligobenzoate molecules in the columnar phase is the aromatic region of the two-dimensional DQ spectrum. Based on the liquid-state ^{1}H NMR spectrum, in which three aromatic resonances at $\delta=8.35$ (Ⓐ), 7.37 (Ⓑ) and 7.42 ppm (Ⓒ) are resolved (Figure 6b), only a single DQ coherence between H_A and H_B at $\delta=15.72$, 8.35–7.37 ppm should be observed in this region of the DQ spectrum because the aromatic protons (H_C) of the outer $OC_{12}H_{25}$-substituted phenyl ring are too far from the nearest aromatic protons to be involved in DQ coherences for short DQ excitation times ($t_{exc}=33.6$ μs). However, the ^{1}H–^{1}H DQ correlation NMR spectrum exhibits a complex pattern in the aromatic region. Local maxima are found for the expected (H_A–H_B) DQ coherence at $\delta=15.4$ (8.2 + 7.2) ppm, the chemical shift values of which were already slightly shifted to lower ppm values, and also at $\delta=14.5$ (7.8 + 6.7) ppm, where every single proton site then experiences a high-field shift of about 0.6 ppm. The high-field shift of the aromatic resonances can be explained by the spatial proximity of the proton sites to aromatic ring currents that, depending on the distance and the orientation of the proton site with respect to the plane of the aromatic π-electron system, causes an additional shift in the range of +0.2 to −1.5 ppm.[34] In the two-dimensional DQ NMR spectrum, the dashed lines parallel to the diagonal of the spectrum (solid diagonal line) indicate the expected positions of H_A–H_B DQ coherences, if both aromatic proton sites experience the same shift owing to their spatial proximity to aromatic π-electron systems. Ridges along these lines would be expected in a heterogeneous distribution of packing arrangements of the benzoate chains. The presence of local maxima on these lines indicates that preferred packing arrangements are found in the sample. However, the chemical shift information alone is not sufficient to propose such packing arrangements.

In contrast to the discussion above, the local maximum at $\delta=14.1$ (7.3 + 6.9) ppm does not follow the dashed lines. In fact there are different ways to interpret this signal: it could result from local packing in which H_A and H_B experience significantly different π-shifts or from local packing with a spatial proximity between H_B and H_C as a result of substantial bending of the oligobenzoate branch.

It should be noted that neither the signals of the aliphatic chains nor the signals of the OCH_2 groups show a noticeable influence on the π-shift distributions, which indicates nano-segregation between the benzoate branches and the aliphatic side-chains. The quality of this nano-segregation is directly reflected in the two-dimensional DQ spectrum. In a perfectly segregated system, the excitation of DQ coherences between aromatic and aliphatic protons should not be feasible. However, in Figure 6a the signal at $\delta=8.5$ (7.2 + 1.3) ppm demonstrates the presence of a spatial proximity between H_B, H_C and the protons of the aliphatic chain of within 0.4 nm, which may be explained by back-folding of the aliphatic chains if it would have been only a weak signal. In fact, the substantial intensity of this signal disproves the assumption of perfect nano-segregation. The weak DQ signal at $\delta=9.5$ (8.2 + 1.3) ppm, which has to be assigned to a DQ coherence between aromatic H_A and an aliphatic proton, finally indicates that any nano-segregation is not compatible with the assumption of a planar arrangement of the star-shaped oligobenzoate molecules with the central phloroglucinol ring located in the centre of the aromatic columns.

In comparison with ^{1}H DQ NMR spectroscopy, deuteron NMR spectroscopy in the solid state is not as sensitive to local packing, but it does provide detailed information on dynamic processes. This is of particular interest in LC systems or soft crystals. Therefore, the dynamic behaviour of

1e was studied by heating the sample from the solid phase at $T=300$ K to the isotropic phase at $T=330$ K. Deuteration of the central ring was chosen because it assembles all three benzoate arms, and therefore, reflects the overall mobility of the molecule. The spectra measured are shown in Figure 7. At room temperature, a typical static powder line

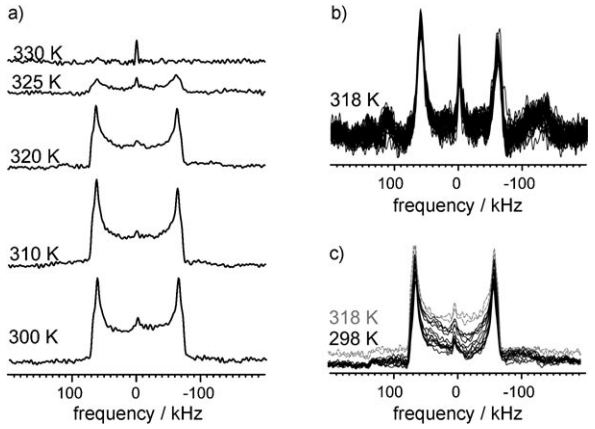

Figure 7. a) ^{2}H NMR spectra of **1e** recorded on heating (solid echo, 25 μs echo delay). b) 45 ^{2}H NMR spectra recorded over a period of 90 h while cooling from the isotropic phase to $T=318$ K. c) Twelve ^{2}H NMR spectra recorded over a period of 24 h at 298 K, with the two last spectra taken again at $T=318$ K.

shape with a quadrupolar coupling $\delta_Q=136$ kHz and asymmetry parameter $\eta=0.07$ is observed. Heating to $T=320$ K led to only a minor drop in intensity. On further heating, an isotropic line appears in the centre of the spectrum that coexisted at $T=325$ K with a remaining part of the powder line shape visible mainly at the position of the singularities. The singularities completely vanish on heating to $T=330$ K. While cooling from the isotropic phase to $T=318$ K (Figure 7b), only the two singularities with a slightly reduced splitting of $\delta_Q=120$ kHz and a remaining broadened isotropic line are observed, which indicates a highly mobile state with isotropic molecular tumbling and a broad distribution of correlation times. Although a static powder line shape has been detected at the same temperature in the heating run, the highly mobile state is stable for at least 90 h. The highly mobile phase returns slowly (within 24 h) to the solid phase only after cooling to $T=298$ K (Figure 7c). This observation is in agreement with the monotropic nature of the columnar hexagonal mesophase.[23c]

It should be noted that the molecular motion of the central phloroglucinol ring in the mobile phase is not rotation around the C_3-symmetry axis of the molecule, as expected for a star-shaped conformation of the molecule, but rather librational dynamics with a broad distribution of correlation times.[35] This type of motion only leads to a minor reduction in the quadrupolar splitting in the slow motion regime, cannot be observed in the intermediate motion regime and appears to be isotropic at the fast motion limit. The observed dynamic behaviour, however, is consistent with the proposed *E*-shaped conformation of the molecule.

In summary, the overall molecular mobility of **1e** is low and not well-defined. Only in the hexagonal phase, after cooling from the isotropic liquid, librational dynamics may explain the low intensity of the signals in ^{2}H solid-state NMR spectroscopy. The deuterated core in the soft crystal phase is almost solid. In contrast, the intensity distribution of the DQ spectra in the same phase clearly shows segment mobility of the aliphatic chains and aromatic building blocks. Although most of the aromatic units and aliphatic chains are nano-segregated, which is determined from the absent influence of π-shift distributions on CH_2, CH_3, or OCH_2 groups, the strong signals for DQ coherence between aromatic and aliphatic protons clearly points to spatial proximity of such protons. Thus, nano-segregation is not perfect, even in the soft crystal phase.

Dilatometry and model of the LC phases: Dilatometry is an important tool that has been used to support structural studies on lyotropic and thermotropic liquid crystals, which assumes that nano-segregation is the driving force of self-assembly.[36] Mesogens **1**, **2** and **3** consist of an aliphatic periphery and a polar benzoate core. Previous results point to nano-segregation as the driving force for molecular assembly because only mesogens with the right number of long alkoxy chains form liquid-crystal phases.[18,37] Thus, the unit cell volume V_{cell} is the sum of the volumes of the polar core and the aliphatic chains. Because the latter is known,[18,38] the volume of the benzoate cores can be estimated in the different mesophases by measuring the molecular volume V_m by dilatometry. In this case, the number of molecules (Z) in a columnar unit or the unit cell can be obtained from the quotient $V_{cell}/V_m=hS/V_m$ (in which $h=$height of the unit cell, $S=$cross-section of the unit cell). V_{cell} is calculated from X-ray data. In the orthorhombic unit cell (Col_{borh}), Z amounts to $Z=abc/V_m$. The height h in the hexagonal unit cell is not known and consequently, V_{cell} and Z are not easily available. For this reason, we have chosen an arbitrary value h, for which a molecular equivalent Z is calculated by $Z=ha^2\sin60°/V_m$. Note that only for the sake of comparison, h is kept constant at 4.5 Å for all compounds in their hexagonal columnar phases. Table 4 lists the dilatometry results for the different phases of compounds **1a** and **1b**. The corresponding graphs can be found in the Supporting Information.

Comparing the phases with the same structure (Col_h for **1a** and **1b**) and at the same temperature, the volume of three benzoate units is estimated to be approximately 433 Å^3. From the temperature-dependence of compound **1b**, the molecular volume of the larger mesogens can be estimated as shown in Table 4. The data is discussed in more detail below in which models for the different phases are developed, based on X-ray diffraction, dilatometry and solid-state NMR spectroscopy results.

*Body-centred orthorhombic columnar soft crystal phases of **1a** and **3***: A model of the low-temperature phase of **1a** has been previously presented based on a hexamer cluster heli-

Table 4. Dilatometry results for **1a** and **1b**, and estimation of molecular volumes of **1c** and **1d**.

Compound[a]	T [°C]	V_m [Å^3]	Z (h [Å])	Temperature dependence [c] [Å^3]
1a (soft Cr$_{borh}$)	31	4080	22.9 (34.0)	$2.695T+3995.9$
1a (Col$_h$)	40	4117	1.7 (4.5)	$2.864T+4002.2$
1b (Col$_{borh}$)	60	4620	23.2 (30.4)	$0.972T+4561.8$
1b (Col$_h$)	91	4707	2.1 (4.5)	$3.121T+4422.5$
1c (Col$_{borh}$)	150	5128[b]	35.5 (37)	–
1c (Col$_h$)	171	5376[b]	2.4 (4.5)	–
1d (Col$_{borh}$)	190	5587[b]	49.3 (43)	–
1d (Col$_h$)	247	6056[b]	2.7 (4.5)	–

[a] Dilatometry was not performed for compound **3**. Because molecules **1a** and **3** only differ by the inverted inner carboxy group, their molecular volumes are assumed to be identical. [b] The molecular volume is estimated from the temperature dependence of **1b** and the volume increment for three benzoate units, which amounts to ≈433 Å^3. Thus, for example, V_m(**1c**, Col$_h$) = (3.121T+4422.5+433) Å^3; in which T = 171 °C V_m = 5376 Å^3. [c] T in °C.

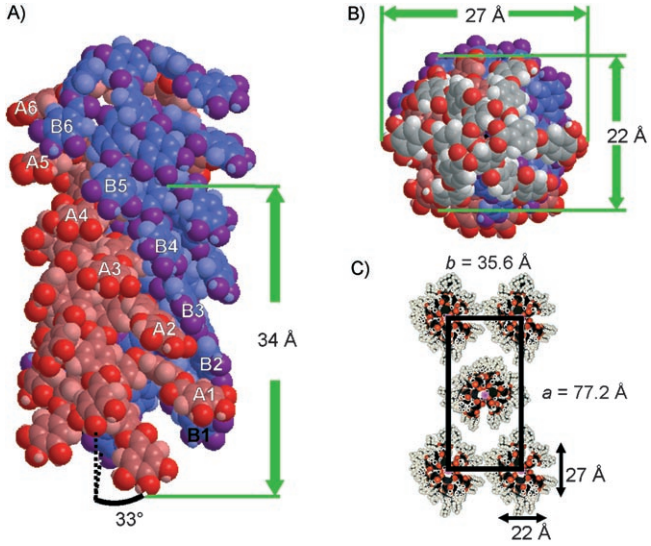

Figure 8. Model of the self-assembly in the soft crystal phase of **1a**. A) Side view of the double helix. B) Top view of the column. C) Columns represented by dimers of a CPK model. Section through the unit cell (a,b plane, c = 0).

cally packed in the column.[23a] This model is in agreement with density measurements, X-ray data and AFM pictures. However, aliphatic chains mix intensively with the polar core of the columns. Herein, we develop a helical model based in principal on a dimer of *E*-shaped molecules. Density measurements give a molecular volume of 4079 Å^3 for the soft crystal phase at 31 °C. Thus, 22.9 molecules fill the repeating unit of the body-centred orthorhombic unit cell. As the unit cell contains two columns, 11 mesogens form a column with a length of 34 Å, which is the periodicity along the column. How can these mesogens be arranged into a columnar structure with a minimised packing energy, that is, with maximum nano-segregation and space-filling? At the halo a set of four maxima (Figure 4) indicates that the mesogens are inclined by 60° versus the columnar axis with an intra-columnar separation of 4.4 Å. The repeat unit of 34 Å along the column clearly shows a 3D periodicity and might be explained with a helical arrangement, which is frequently reported for star-shaped molecules.[11a,b,15a,b] The high order of the mesostructure and solid-state NMR spectroscopy results indicate that a certain conformer constitutes the building block. As discussed recently, a large number of different conformers are possible for these semi-flexible star-mesogens.[19] If star-shaped molecules arrange in a similar manner to those recently reported for the crystal structure of a derivative with short chains, in which space filling dominates, then 11 mesogens on top of each other would result in a column with a length of 11×4.4 Å = 48.4 Å.[39] This result shows that the column must comprise more than one molecule in the columnar unit of a thickness of 4.4 Å. If we assume nano-segregation as the main driving force towards the supramolecular structure, then a dimer of *E*-shaped conformers can segregate aliphatic chains and the benzoate core and efficiently fill the space. A model of a possible arrangement is given in Figure 8A and B. The *E*-shaped conformer is inclined by 60° and covers an azimuthal angle of about 169°. A pair of mesogens (red and blue) form a dimer. One of the mesogens (blue) is offset by 3.1 Å along the column direction and the pairs of molecules are separated by 6.2 Å.[40] The next dimer is rotated by 33°.[41] This leads to a double helix with a red (A1–A6) and a blue (B1–B6) strand. The model explains the repeating unit along the column because the first *E*-conformer (B1) of the blue helix is at the same angular position as the sixth mesogen (A6) of the red helix. The periodicity is then (5×6.2)+3.1 Å = 34.1 Å because the blue and the red strand are offset by 3.1 Å. Thus, the unit cell contains 5.5 mesogens from the blue strand and 5.5 from the red strand, which is in agreement with X-ray and dilatometry data. The arrangement of dimers (CPK model) in the unit cell is shown in Figure 8C. The benzoate core has a length of approximately 27 Å and a breadth of 22 Å. The column in the middle is shifted by c/2, thus the long half-axis of the elliptical cross-section is rotated by 90° versus the long half-axes of the four other columns (Figure 5). The aliphatic chains are in a liquid state and not necessarily inclined with respect to the column axis, and consequently, may fill the free space.

Compound **3** is distinguished from **1a** only in the inverse inner carboxy groups. This small detail leads to a significant change in the transition temperatures, although the packing behaviour seems to be similar to that of **1a**. The soft crystalline phase is characterised by a body-centred orthorhombic unit cell (Table 3). The columnar structure remains upon crystallisation by annealing, which is evidenced by the X-ray diffractogram of an aligned enantiotropic hexagonal phase after the transition from the soft crystal (see the Supporting Information). The packing of the undulated columns in the a,b plane is slightly different from **1a**, and the repeating unit along the column axis is increased by a factor of two (i.e., 64.6 Å). The number of molecules per columnar unit also doubles and amounts to approximately 24 mesogens, if the same molecular volume as for **1a** is assumed. The diffuse set

of four reflections at the meridian point to an inclination of the molecules by only 30°; the smaller tilt of the mesogens may be attributed to the larger planar core of the trimesic acid centre. A helical organisation can be rationalised by 12 dimers separated by 5.4 Å and rotationally displaced by 30°. In contrast to compound **1a**, the periodicity relates to a full turn of the double helix.

*Body-centred orthorhombic columnar liquid-crystal phase of **1b–d***: X-ray diffraction of the extended oligobenzoates shows diffraction patterns with similar features as those obtained with **1a** or **3** (see the Supporting Information); 1) the mesogens are inclined by almost 60°, 2) the reflections on the equator can be attributed to a rectangular organisation of columns and 3) the set of four signals at the meridian can be indexed according to (211) planes. Thus, the LC unit cells are described as body-centred orthorhombic cells and contain two undulated columns, which are formed by approximately 12, 18 and 24 molecules per column in **1b**, **1c** and **1d**, respectively. It is evident that the number of molecules per columnar unit increases more rapidly than the height of the unit cells (30.4, 37.0, 43.0 Å, see Table 3). This observation can be rationalised if more molecules are needed to form a columnar slice of a defined thickness with larger column diameter. Although the length of the individual arms, and therefore, the diameter of the columns increases from **1a** to **1d**, the volume of the peripheral groups remains the same. Consequently, when the benzoate groups in the centre increase the radius of the column, a single molecule occupies a smaller columnar fraction, which is reflected by the decreasing angle enclosed by the two folded arms of the *E*-shaped conformer with increasing size of the mesogens (Figure 9). The number of molecules needed to pack into a columnar slice thus increases.

*Hexagonal columnar phase of **1a** and **3***: The WAXS pattern of **1a** of a freshly extruded fibre shows not only hexagonal lattice symmetry, but also two other interesting features. The increased intensity at the halo is very broad and the intensity is highest at the meridian, which indicates that the mesogens are, on average, oriented orthogonally to the columnar axis and are no longer regularly inclined. The small-angle meridional peak, which was relatively intense and sharp for the orthorhombic helical phase (17 Å, $\xi d^{-1}=20$ repeating units), is now diffuse and shifted to a Bragg distance of 19.3 Å. Consequently, a periodicity along the columns still exists in the hexagonal phase, but with a very small correlation length ξ of approximately three repeating units. This is probably rationalised by a preceding helical order before the material transforms into the low-temperature phase.

These features can also be observed for the hexagonal phase of **3**. On heating the soft crystal to 80 °C, the helical arrangement disappears. At 80 °C, no meridional reflection can be determined in the X-ray pattern of the hexagonal phase. Nevertheless, if the Col_h phase is supercooled, a meridional reflection is present at room temperature, which indicates periodicity along the columns and which may be rationalised by a helical preorganisation. Similar to **1a**, the related Bragg distances of the meridional reflections increase from 32.3 Å in the orthorhombic cell to 37.9 Å in the hexagonal cell at room temperature. The smaller distance in the rectangular helical soft crystal points to optimised packing compared to the hexagonal phase.

Interestingly, the hexagonal cell parameters are of the same size for both molecules. This may raise the question as to whether the same type of conformers participates in the molecular assembly. Before tackling the latter problem, a model based on nano-segregation should be discussed for **1a** that visualises the size of cross-sections for benzoates and aliphatic chains. The results are shown in Figure 10; the detailed calculations can be found in the Supporting Information.

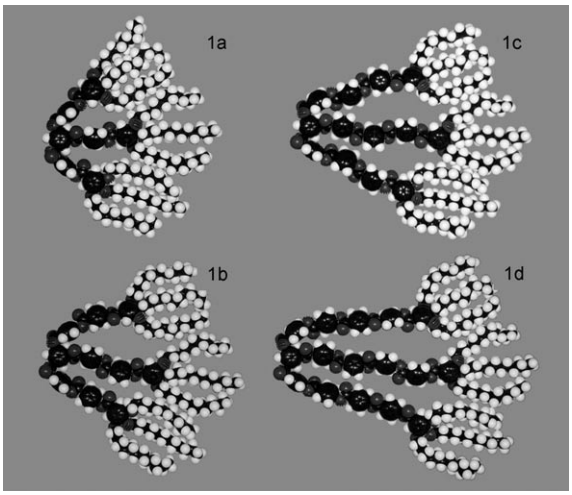

Figure 9. *E*-shaped conformers of oligobenzoates (CPK models) based on a phloroglucinol core.

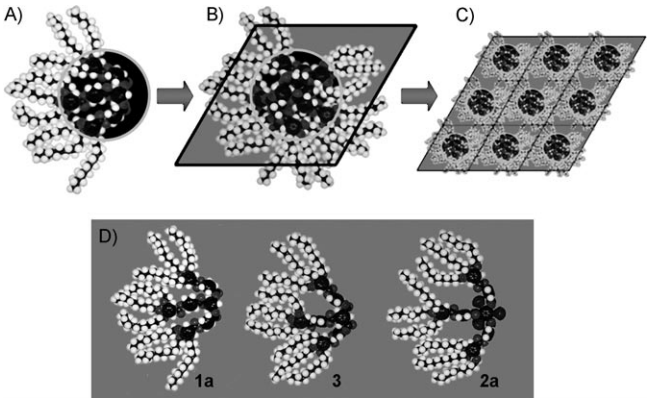

Figure 10. Model of the hexagonal phase. A) *E*-shaped conformer of **1a**. The dark grey background with the light grey circle indicates the cross-section of the benzoate core of a column. B) Possible organisation of two molecules of **1a**. The lines highlight the hexagonal unit cell and the light grey background shows the cross-section of the aliphatic chains. C) Assembly of nine unit cells. The free space on the upper part of the cell is filled by segments of molecules positioned below the conformer in A. D) *E*-shaped conformers of **1a**, **3** and **2a**.

The black area with the light grey border corresponds to the cross-section of the core of the column filled with benzoates. The grey background of the hexagonal unit cell is the cross section of the aliphatic chains. The model demonstrates that a single *E*-shaped conformer cannot fill the space of such a columnar slice as shown in Figure 10. Therefore, about 40% of the cell ($h=4.5$ Å) is occupied by molecules below and above the reference mesogen in panel A, which is probably the driving force towards the helical preorganisation in the hexagonal phase. Only a folded conformer, such as the *E*-shape type, can account for all of the observed features: 1) the small benzoate diameter of the column, 2) the number of molecules per columnar slice, 3) no large angle mobility (rotation) of mesogens in the liquid-crystal phase owing to the fact that the centre of mass does not coincide with the centre of the column and 4) the helical structures.

As discussed earlier, the core of **3** is larger than that of **1a** owing to conjugation between the carboxy groups and the central benzene. Nevertheless, the column diameters are the same for the mesogens. Figure 10D shows *E*-shaped conformers (CPK models) of molecules **1a** and **3**. Mesogen **3** can adopt such a conformer in spite of the larger planar core.

*Hexagonal columnar phases of **1b–d***: Owing to transesterification reactions of **1c** and **1d** in their hexagonal phases at high temperatures, the cell parameters of previously published synchrotron results are used for the following analysis.[18a] Similar to **1a**, the meridional diffuse intensity for **1b** (22.4 Å, $\xi d^{-1}=5.4$ repeating units) points to a helical preorganisation of mesogens. We assume a closely related self-organisation for **1c** and **1d**, as a consequence of the similar structures for the low-temperature phases of **1a–d**. Table 5 summarises the core radii of these compounds obtained from dilatometry and X-ray studies. As emphasised earlier, the radius of the benzoate core of the column is much smaller than the radius of a C_3-symmetric star-shaped conformer (Table 5, entries in the last column). The length of the benzoate segment of the *E*-shaped conformers, $r_{E\text{-shape}}$, is smaller than the radius of the column core. This is in agreement with the model presented in Figure 10 in which molecules from below and above the reference mesogen contribute to the columnar slice. The calculated number of molecules in the columnar unit for **1b** and the estimated values for **1c** and **1d** (Table 4) show that Z increases from 1.7 (**1a**) to 2.8 (**1d**). As the periphery of these mesogens always contains three gallic acid derivatives, they occupy a segment on the circumference of the circular cross-section of the Col_h phase with constant length L. The circumference of a circle increases with $2\pi r$ and should contain Z molecules, thus $LZ=2\pi r$. In the hexagonal phases with a circular cross-section of the column cores completely surrounded by peripheral alkoxy-substituted groups, a linear relationship between the number of molecules in a columnar slice Z and the radius r is expected, namely, $Z=2\pi rL^{-1}$. The diagram in Figure 11 presents an excellent linear correlation between the experimental radius of the core and the number of molecules in a columnar slice with a height of 4.5 Å. Comparison of the ideal curve (dashed line), in which the interface between the aliphatic and benzoate segments is formed by peripheral units, with the experimental curve (solid line) shows that the experimental number of molecules contained in a columnar slice increases less rapidly than proposed. The mismatch between the columnar radius and the number of molecules Z becomes larger as the length of the oligobenzoate arms increases. This is related to the fact that the oligobenzoates of one molecule fill a larger fraction of the columnar core than the alkoxy groups at the periphery. The inset of Figure 11 shows a model for mesogens **1a**, in which individual molecules occupy a segment of a columnar slice. This model

Table 5. Comparison of the experimental radius of the benzoate core of the column with the measured radius of *E*-shaped and C_3-symmetric star-shaped mesogens.

Compound	$r_{\text{benzoate core}}$	$r_{E\text{ shape}}$	r_{C3stars}
1a	11.8	8.9	15.2
1b	16.0	11.9	21.7
1c	20.0	15.0	28.2
1d	23.3	18.1	34.6

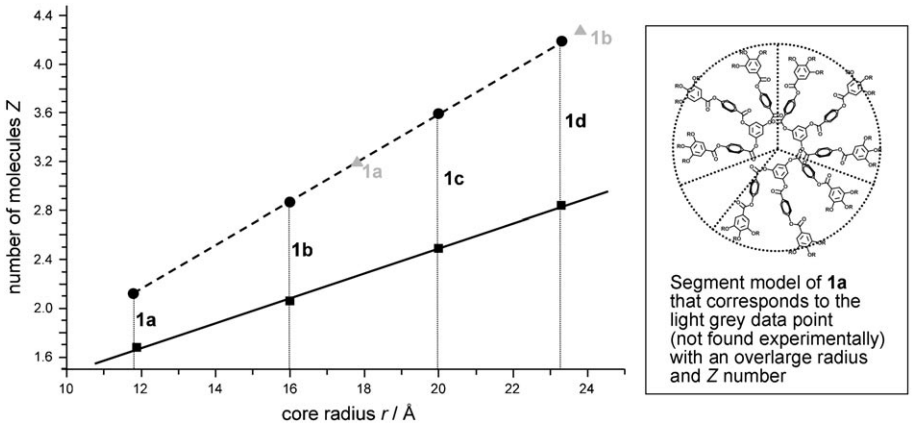

Figure 11. Relationship between the benzoate core radius r and the number of molecules Z in a columnar slice for mesogens **1a–d**. Experimental data (■) and the fit function for $Z=0.458\pm0.046+(0.102\pm0.002)r$ ($R=0.9994$) (——) are shown. The ideal relationship when the peripheral units of an *E*-shaped molecule perfectly cover the interface between the aliphatic chains and the oligobenzoate core ($Z=2\pi r/L=0.180r$ with $L=35$ Å) is also shown – – –. The parameter L is taken from a molecular model of **1a**. The inset illustrates a hypothetical segment model, in which *E*-shaped molecules pack in segments of a circular columnar slice, and therefore, optimise the nano-segregation. Much larger radii and numbers of molecules Z should be expected (▲).

would optimise nano-segregation; however, a void remains in the centre of the column. Moreover, such a model would predict much larger numbers Z per columnar slice and larger core radii, which are not found experimentally (▲ in Figure 11). Consequently, the experimental data indicates that the peripheral gallic acid residues cannot perfectly cover the interface between aliphatic chains and oligobenzoates, which is in agreement with the results from solid-state NMR spectroscopy that demonstrate non-perfect nano-segregation. The self-assembly of these non-conventional mesogens is obviously governed by a compromise between nano-segregation and space filling.

*Hexagonal columnar phases of **2a** and **2b***: Compounds **2a** and **2b** have been designed to hinder the formation of folded conformers. Indeed, the central benzoate units have to rotate 90° out of the molecular plane. Such steric hindrance has been thought to prevent the formation of liquid crystals. Nevertheless, compounds **2a** and **2b** assemble in columnar liquid-crystal phases, which possess almost the same thermal stability as related mesogens **1**. Obviously, the impact of steric congestion from the iodine atoms on columnar aggregation is small. Moreover, it is surprising that parameters a for the hexagonal unit cells of **2a** or **2b** are again identical to those of **1a** and **3** or **1b**, respectively. Because the central benzoates are forced into a C_3-symmetric inner part of the mesogen in the AM1-minimised model (Figure 2), larger radii comparable to the values of $r_{C3stars}$ in Table 5, and consequently, larger column diameters were expected. In contrast, the column diameters of **2a** and **2b** are comparable to the diameters of **1a** and **1b**, respectively, and can be rationalised with *E*-shaped conformers. Figure 10D shows that such conformers are indeed reasonable for molecules with a triiodophloroglucinol core. The two lateral arms enclose a wider angle than those of mesogens **1a** or **3**. For this reason, the benzoate core becomes broader. The size of mesogen **2a** increases to ≈28 Å, which is larger than the diameter of the column core measured for **1a**. This is evidently compensated by a 43° tilt of the mesogens in the LC phase, which is confirmed by the X-ray pattern. The butterfly pattern at small angles points to a helical arrangement of mesogens (Figure 4C). In contrast to **1a**, the Col_h phase of **2a** is enantiotropic. An analogous behaviour has been observed for mesogen **2b**.

Packing motifs—theoretical considerations: The optimum relative orientation of star-shaped mesogens within a columnar stack was investigated with the help of density-functional-based tight-binding calculations[42], and included dispersion interaction between non-covalently bonded molecules or fragments.[43] This approach has already been successfully applied to analyse stacking of the more rigid and ideally planar 1,3,5-tris-pyrazolylbenzene derivatives in columnar phases.[44] A similar analysis for the present star-shaped mesogens with a phloroglucinol core and oligobenzoate arms is more difficult owing to the higher flexibility and non-planarity of the molecules. Hence, the thorough analysis of the single star-shaped mesogens yielded the core structure of **1a** in good agreement with experimental crystal structure data,[19,21] but only limited information could be obtained on the preferred conformation and orientation of such a mesogen within a columnar phase.

Of special interest is the relative rotation angle ϕ between two adjacent mesogens along the column, which can give rise to a helical order. The theoretical investigation of this quantity was performed in a two-step process: the lower relative rotation angles $\phi < 20°$ were studied with the help of a non-periodic stack of four molecules. For larger values of ϕ, a periodically repeated stack was employed that consisted of $N = 360°/\phi$ molecules or $120°/\phi$ for the threefold-symmetric structures. The simulations were performed for several fixed average intermolecular distances along the stack, ranging from 3 to 6 Å. Both the three-fold symmetric star-shaped molecule and the less symmetric folded star in the *E* conformation were studied. Figure 12 shows the relative total energies per single mesogen as a function of the rotation angle ϕ; the energy of the most stable arrangement was chosen as the reference. Figure 12A displays the values calculated for the nearly planar three-fold symmetric stars, and Figure 12B shows the curves for stacks of non-planar folded mesogens. In both cases, the curves for the experimental intermolecular distance of ≈4.4 Å is displayed (– – – in Figure 12) along

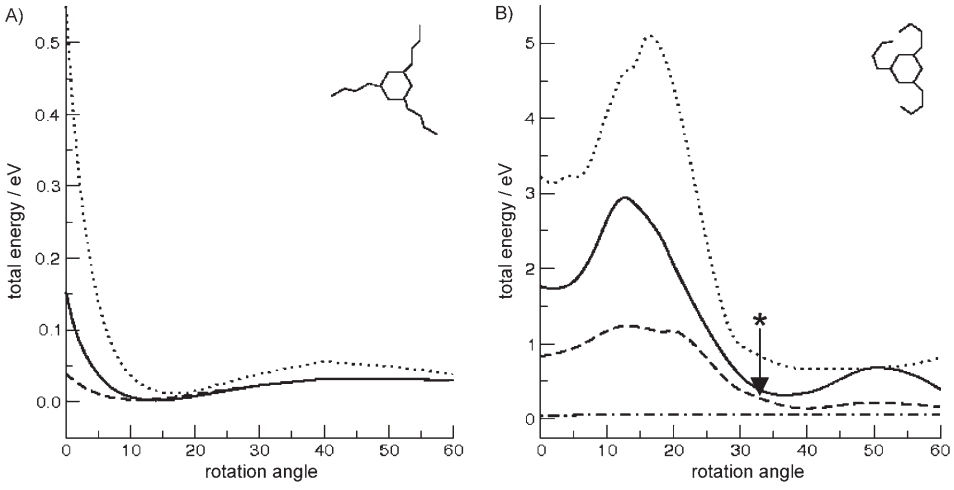

Figure 12. Relative total energies per mesogen in a stack of four molecules as a function of the rotation angle ϕ at various intra-stack distances; results from periodic calculations are included from 20° onward. A) Calculations for C_3-symmetric conformers at 3.6 (•••••), 4.0 (——) and 4.4 Å (– – –). B) Calculations for *E*-shaped conformers at 3.6 (•••••), 4.0 (——), 4.4 (– – –) and 6.0 Å (–•–•); the value proposed by the model best fitting the experimental results is also indicated (*).

with other prototypical distances. The most stable structure for a single column is formed by three-fold symmetric mesogens with an intermolecular distance of 4.4 Å and a rotation angle ϕ of 12°, that is, with about 10 molecules along the repeat unit of the column. However, other threefold-symmetric arrangements with ϕ values between 10 and 20° and oscillations of the intermolecular distances between 4 and 5 Å are energetically very close, so that they may also be stabilised by packing and/or template effects. It is equally likely that the same mechanisms can stabilise a stack of deformed mesogens, as displayed in Figure 12B, although the angle dependence is more severe at the experimental intermolecular distance. Yet, with an optimum angle of 35°, stable stacks are obtained that are consistent with the analysis of the experimental data. Deviations from helical stacking are disfavoured by energy barriers of at least 0.04 eV per molecule at $\phi = 0°$ (or 60°) at the experimental intermolecular distance.

Conclusion

Non-conventional star-shaped mesogens with various cores (phloroglucinol, triiodophloroglucinol and trimesic acid) and different benzoate arm lengths have been synthesised. The compounds form high-temperature hexagonal phases (Col_h) and low-temperature orthorhombic body-centred phases (Col_{borh}) or soft crystals (Cr_{borh}). Dilatometry, X-ray diffraction data and solid-state NMR spectroscopy results of a core-deuterated derivative are in agreement with a model of undulated columns formed by a helical arrangement of tilted *E*-shaped conformers in the orthorhombic soft crystal and columnar liquid crystal. The data indicate that the material does not undergo perfect nano-segregation, instead, nano-segregation and space-filling are two competing factors in the self-organisation of star-shaped oligobenzoates. Benzoate core diameters in the hexagonal phases can be estimated and the small values also point to *E*-shaped conformers. The different electronic and steric effects of the various central building blocks do not affect the benzoate core diameters, they only affect the mesogen tilt with respect to the column axis. Interestingly, X-ray diffraction data point to a helical preorganisation of mesogens in the Col_h phase. Only in derivative **3**, in which the existence of the hexagonal columnar phase extends over a large temperature interval of 54 °C, the intracolumnar preorganisation disappears close to the clearing temperature.

Experimental Section

General: Chemicals were obtained from Acros and Sigma-Aldrich and were used as received. The synthesis of compounds **1a** to **1d** was described previously.[19] Column chromatography was carried out on silica 60 gel (Merck, mesh 70–230). PFT ^{1}H and ^{13}C NMR spectra were recorded in $CDCl_3$ by using Varian 300 MHz and Varian Oxford 400 MHz spectrometers with the residual solvent signal at $\delta = 7.26$ ppm as a reference. Mass spectra were obtained by using a Finnigan MAT95 (FD MS) instrument. Elemental analyses were carried out in the microanalytical laboratory at the University of Mainz (Germany).

X-ray diffraction: The WAXS measurements of aligned samples obtained by extrusion were made with a standard copper anode (2.2 kW) source with a pinhole collimator equipped with an X-ray mirror (Osmic type CMF15-sCu6) and a Bruker detector (High-star) with 1024×1024 pixels. The SAXS measurements of aligned samples were performed with a rotating anode (mikromax 007, copper, Rigaku) source with a pinhole collimator equipped with an X-ray mirror (Osmic type 140–004012) and a Bruker detector (High-star) with 1024×1024 pixels. Calibration was performed with silver behenate.[45] The X-ray patterns were evaluated with the datasqueeze software.[46] The correlation length was determined by using the Scheerer formula and the half-width and reflection maximum were obtained from the fit function.

1,3,5-Tris-[4-(3,4,5-tridodecyloxybenzoyloxy)benzoyloxy]-2,4,6-trideuteriobenzene (1e): Compound **5** ($n = 1$; 1.5 g, 1.89 mmol), 1,3,5-trihydroxy-2,4,6-trideuteriobenzene (0.08 g, 0.60 mmol),[47] dicyclohexylcarbodiimide (DCC; 0.79 g, 3.77 mmol) and 4-dimethylaminopyridinium toluylsulfonate (DPTS; 0.22 g, 0.76 mmol) were dissolved in dry CH_2Cl_2 (10 mL) and stirred at ambient temperature overnight. The solvent was removed and the product was extracted with hexane. Evaporation of the solvent and recrystallisation from acetone gave a colourless waxy solid (1.05 g, 74 %). The degree of deuteration was 95 %. ^{1}H NMR (400 MHz, $CDCl_3$): $\delta = 0.88$ (t, 27 H; CH_3), 1.26–1.53 (m, 162 H; CH_2), 1.73–1.88 (m, 18 H; CH_2), 4.06 (2 t, 18 H; OCH_2); 7.20 (residual proton signal of the core, 0.15 H), 7.37 (AA′BB′, 6 H; ArH), 7.41 (s, 6 H; ArH); 8.29 ppm (AA′BB′, 6 H; ArH); ^{13}C NMR (100 MHz, $CDCl_3$): $\delta = 14.1$ (CH_3), 22.7–31.9 (CH_2), 69.3, 73.6 (OCH_2), 108.6 (Ar CH), 113.1 (br; Ar CD), 122.2 (Ar CH), 123.2, 126.5 (Ar C_q), 131.9 (Ar CH), 143.3, 151.4 153.0, 155.5 (Ar C_q), 163.7, 164.4 ppm (C=O); FD MS: m/z (%): 2460.3 (100, $[M+1]^+$); elemental analysis calcd (%) for $C_{156}H_{243}D_3O_{21}$: C 76.15, H 10.20; found: C 75.94, H 10.08.

1,3,5-Tris(3,4,5-tridodecyloxybenzoyloxy-4′-benzoyloxy)-2,4,6-triiodobenzene (2a): Compound **5** ($n = 1$; 150 mg, 0.19 mmol), 2,4,6-triiodophloroglucinol **4** (X = I; 31 mg, 0.06 mmol), DCC (230 mg, 0.28 mmol) and DPTS (10 mg, 0.04 mmol) were dissolved in dry CH_2Cl_2 (10 mL) and stirred at ambient temperature overnight. The solvent was removed and the product was purified by column chromatography (silica gel, hexane/ethyl acetate). Recrystallisation from acetone gave a colourless waxy solid (126 mg, 72 %). T_{Cl} (clearing temperature; onset DSC) = 58 °C; ^{1}H NMR (300 MHz, $CDCl_3$): $\delta = 0.86$, 0.88 (2 t, 27 H; CH_3), 1.26–1.55 (m, 162 H; CH_2), 1.80 (m, 18 H; CH_2), 4.06, 4.08 (2 t, 18 H; OCH_2), 7.416 (AA′BB′, 6 H; ArH), 7.421 (s, 6 H; ArH), 8.38 ppm (AA′BB′, 12 H; ArH); ^{13}C NMR (100 MHz, $CDCl_3$): $\delta = 14.1$ (CH_3), 22.7–31.9 (CH_2), 69.3, 73.6 (OCH_2), 86.0 (Ar C_q), 108.6, 122.3 (Ar CH), 123.2, 125.9 (Ar C_q), 132.4 (Ar CH), 143.3, 153.0, 154.3, 155.8 (Ar C_q), 161.6, 164.4 ppm (C=O); FD MS: m/z (%): 2835.2 (100, $[M+1]^+$); elemental analysis calcd (%) for $C_{156}H_{243}I_3O_{21}$: C 66.08, H 8.64; found: C 66.12, H 8.55.

1,3,5-Tris(3,4,5-tridodecyloxybenzoyloxy-4′-benzoyloxy-4″-benzoyloxy)-2,4,6-triiodobenzene (2b): Compound **5** ($n = 2$; 172 mg, 0.19 mmol), 2,4,6-triiodophloroglucinol **4** (X = I; 31 mg, 0.06 mmol), DCC (230 mg, 0.28 mmol) and DPTS (10 mg, 0.04 mmol) were dissolved in dry CH_2Cl_2 (10 mL) and stirred at ambient temperature overnight. The solvent was removed and the product was purified by column chromatography (silica gel, hexane/ethyl acetate). Recrystallisation from acetone gave a colourless waxy solid (126 mg, 66 %). T_{Cl} (onset DSC) = 82 °C; ^{1}H NMR (400 MHz, $CDCl_3$): $\delta = 0.879$, 0.883 (2 t, 27 H; CH_3), 1.26–1.88 (m, 180 H; CH_2), 4.06, 4.08 (2 t, 18 H; OCH_2), 7.39, 7,46 (AA′BB′, 24 H; Ar CH), 7.42 (s, 6 H; Ar CH), 8.31, 8.40 ppm (AA′BB′, 12 H; Ar CH); ^{13}C NMR (100 MHz, $CDCl_3$): $\delta = 14.1$ (CH_3), 22.7–31.9 (CH_2), 69.3, 73.6 (OCH_2), 86.0 (Ar C_q), 108.6, 122.3 (Ar CH), 123.2, 126.1, 126.4 (Ar C_q), 132.0, 132.5 (Ar CH), 143.3, 153.0, 154.3, 155.6 (Ar C_q), 161.6, 163.8, 164.4 ppm (CO); FD MS: m/z (%): 3197.2 (100, $[M+2+H]^+$); elemental analysis calcd (%) for $C_{177}H_{255}I_3O_{27}$: C 66.53, H 8.04; found: C 67.02, H 7.90.

1,3,5-Tris(3,4,5-tridodecyloxybenzoyloxy-4′-phenyloxycarbonyl)benzene (3): Compound **7** (205 mg, 0.27 mmol) and **6** (24 mg, 0.09 mmol) were dissolved in dry CH_2Cl_2 (10 mL) and triethylamine (0.2 mL) was added. The mixture was stirred at ambient temperature overnight. The solvent

was removed and the product was purified by column chromatography (silica gel, hexane/ethyl acetate). Recrystallisation from acetone gave a colourless waxy solid (125 mg, 57%). T_{Cl} (Onset DSC) = 88 °C; ^{1}H NMR (300 MHz, $CDCl_3$): δ = 0.92 (m, 27H; CH_3), 1.27 (m, 162H; CH_2), 1.50 (m, 18H; CH_2), 1.81 (m, 18H; CH_2), 4.06, 4.07 (2t, 18H; OCH_2), 7.31 (AA′BB′, 12H; ArH), 7.42 (s, 6H; ArH), 9.27 ppm (s, 3H; ArH); ^{13}C NMR (75 MHz, $CDCl_3$): δ = 14.1 (CH_3), 22.6–31.9 (CH_2), 69.2, 73.5 (OCH_2), 108.5, 122.4, 122.9 (Ar CH), 123.6, 131.1 (Ar C_q), 136.1 (Ar CH), 143.1, 147.9, 148.8, 152.9 (Ar C_q), 163.1, 164.8 ppm (C=O); FD MS: *m/z* (%): 2458.0 (100, $[M]^+$), 1424.2 (77, $[M]^{2+}$); elemental analysis calcd (%) for $C_{156}H_{246}O_{21}$: C 76.24, H 10.09; found: C 75.88, H 9.89.

Acknowledgements

We thank Prof. H. Meier, A. Oehlhof and Dr. N. Hanold for the elemental analyses and FD mass spectra completed at the University of Mainz. The Deutsche Forschungsgemeinschaft (DFG) and the Bundesministerium für Bildung und Forschung (BMBF) are gratefully acknowledged for their financial support.

[1] a) C. Tschierske, *Ann. Rep. Prog. Chem., Sect. C: Phys. Chem.* **2001**, *97*, 191–267, and references therein; b) C. Tschierske, *Prog. Polym. Sci.* **1996**, *21*, 775–852; c) D. Demus, *Liq. Cryst.* **1989**, *5*, 75–110.

[2] a) I. M. Saez, J. W. Goodby, *J. Mater. Chem.* **2005**, *15*, 26–40; b) I. M. Saez, J. W. Goodby, *Chem. Eur. J.* **2003**, *9*, 4869–4877.

[3] a) V. Percec, M. Glodde, M. Peterca, A. Rapp, I. Schnell, H. W. Spiess, T. K. Bera, Y. Miura, V. S. Balagurusamy, E. Aqad, P. A. Heiney, *Chem. Eur. J.* **2006**, *12*, 6298–6314; b) V. Percec, M. Glodde, T. K. Bera, Y. Miura, I. Shiyanovskaya, K. D. Singer, V. S. K. Balagurusamy, P. A. Heiney, I. Schnell, A. Rapp, H. W. Spiess, S. D. Hudson, H. Duan, *Nature* **2002**, *417*, 384–387.

[4] a) B. Donnio, D. Guillon, *Adv. Polym. Sci.* **2006**, *201*, 45–155; b) S. A. Ponomarenko, N. Boiko, V. Shibaev, *Polym. Sci. C* **2001**, *43*,1–45.

[5] a) A. M. Giroud-Godquin in *Handbook of Liquid Crystals* (Eds.: D. Demus, J. W. Goodby, G. W. Gray, H.-W. Spiess, V. Vill), *Vol 2b*, S. 900, Wiley-VCH, Weinheim, **1998**; b) B. Donnio, D. Guillon, R. Deschenaux, D. W. Bruce, *Compreh. Coord. Chem. II* **2004**, ***7***, 357–627; c) R. Gimenez, D. P. Lydon, J. L. Serrano, *Curr. Opin. Sol. State Mater. Sci.* **2002**, *6*, 527–535; d) T. Cardinaels, J. Ramaekers, D. Guillon, B. Donnio, K. Binnemans, *J. Am. Chem. Soc.* **2005**, *127*, 17602–17603.

[6] a) T. Kato, N. Mizoshita, K. Kishimoto, Angew. Chem. **2006**, *118, 44–74; Angew. Chem. Int. Ed.* **2006**, *45*, 38–68; *Angew. Chem. Int. Ed.* **2006**, *45*, 38–68, and references therein; b) C. M. Paleos, D. Tsiourvas, *Liq. Cryst.* **2001**,*28*, 1127–1161.

[7] a) C. Tschierske, *J. Mater. Chem.* **2001**, *11*, 2647–2671; b) C. Tschierske, *J. Mater. Chem.* **1998**, *8*, 1485–1508.

[8] D. Guillon, *Struct. Bonding (Berlin)* **1999**, *95*, 41–82.

[9] A. Skoulios, D. Guillon, *Mol. Cryst. Liq. Cryst.* **1988**, *165*, 317–332.

[10] For some examples of shape-persistent three-armed mesogens, see: a) R. Christiano, D. M. Pereira de Oliveira Santos, H. Gallardo, *Liq. Cryst.* **2005**, *32*, 7–14; b) Y.-C. Lin, C. K. Lai, Y.-C. Chang, K.-T. Liu, *Liq. Cryst.* **2002**, *29*, 237–242; c) C.-H. Lee, T. Yamamoto, *Mol. Cryst. Liq. Cryst.* **2002**, *378*, 13–21; d) B. G. Kim, S. Kim, S. Y. Park, *Tetrahedron Lett.* **2001**, *42*, 2697–2699; e) J. C. Chang, J. R. Yeon, Y. S. Chin, M. J. Han, S.-K. Hong, *Chem. Mater.* **2000**, *12*, 1076–1082; f) J. C. Chang, J. H. Baik, C. B. Lee, M. J. Han, S.-K. Hong, *J. Am. Chem. Soc.* **1997**, *119*, 3197–3198; g) D. J. Pesak, J. S. Moore, *Angew. Chem.* **1997**, *109*, 1709–1712; *Angew. Chem. Int. Ed. Engl.* **1997**, *36*, 1636–1639; .

[11] For some examples of three-armed stilbenoid mesogens, see: a) M. Lehmann, C. Köhn, H. Meier, S. Renker, A. Oehlhof, *J. Mater. Chem.*, **2006**, *16*, 441–451; b) H. C. Holst, T. Pakula, H. Meier, *Tetrahedron* **2004**, *60*, 6765–6775; c) H. Meier, M. Lehmann, H. C. Holst, D. Schwöppe, *Tetrahedron* **2004**, *60*, 6881–6888; d) H. Meier, M. Lehmann, U. Kolb, *Chem. Eur. J.* **2000**, *6*, 2462–2469; e) M. Lehmann, B. Schartel, M. Hennecke, H. Meier, *Tetrahedron*, **1999**, *55*, 13377–13394; f) H. Meier, M. Lehmann, *Angew. Chem.* **1998**, *110*, 666–669; *Angew. Chem. Int. Ed.* **1998**, *37*, 643–645; g) A.-J. Attias, Ch. Cavalli, B. Donnio, D. Guillon, P. Hapiot, J. Malthête, *Chem. Mater.*, **2002**, *14*, 375–384; h) G. Zerban, H. Meier, *Z. Naturforsch. B* **1993**, *48*, 171–184; i) H. Meier, *Angew. Chem.* **1992**, *104*, 1425–1576.

[12] For some examples of hydrogen-bonded three-armed mesogens, see: a) J. Barberá, L. Puig, J.-L. Serrano, T. Sierra, *Chem. Mater.* **2004**, *16*, 3308–3317; b) M. L. Bushey, T.-Q. Nguyen, W. Zhang, D. Horoszewski, C. Nuckolls, *Angew. Chem.* **2004**, *116*, 5562–5570; *Angew. Chem. Int. Ed.* **2004**, *43*, 5446–5453, and references therein; c) J. J. van Gorp, J. A. J. M. Vekemans, E. W. Meijer, *Mol. Cryst. Liq. Cryst.* **2003**, *397*, 191–205; d) J. J. van Gorp, J. A. J. M. Vekemans, E. W. Meijer, *J. Am. Chem. Soc.* **2002**, *124*, 14759–14769, and references therein.

[13] M. Katoh, S. Uehara, S. Kohmoto, K. Kishikawa, *Chem. Lett.* **2006**, *35*, 322–323.

[14] T. Hatano, T. Kato, *Chem. Commun.* **2006**, 1277–1279.

[15] For examples of C_3-symmetric cyclotriphosphazene mesogens, see: a) J. Barberá, J. Jiménez, A. Laguna, L. Oriol, S. Pérez, J. L. Serrano, *Chem. Mater.* **2006**, *18*, 5437–5445; b) J. Barberá, M. Bardjí, J. Jiménez, A. Laguna, M. P. Martínez, L. Oriol, J. L. Serrano, I. Zaragozano, *J. Am. Chem. Soc.* **2005**, *127*, 8994–9002; c) K. Moriya, Y. Kawanishi, S. Yano, M. Kajiwara, *Chem. Commun.* **2000**, 1111–1112; d) A. M. Levelut, K. Morija, *Liq. Cryst.* **1996**, *20*, 119–124.

[16] D. Goldmann, D. Janietz, C. Schmidt, J. H. Wendorff, *Liq. Cryst.* **1998**, *25*, 711–719.

[17] For examples of three-armed star-shaped oligobenzoate mesogens, see: a) B.-Y. Zhang, D.-S. Yao, F.-B. Meng, Y.-H. Li, *J. Mol. Struct.* **2005**, *741*, 135–140; b) F. Y. Fan, S. W. Culligan, J. C. Mastrangelo, D. Katsis, S. H. Chen, *Chem. Mater.* **2001**, *13*, 4584–4594; c) A. Omenat, J. Barberá, J.-L. Serrano, S. Houbrechts, A. Persoons, *Adv. Mater.* **1999**, *11*, 1292–1295; d) B. Liu, X. Y. Zahang, X. Z. Yang, *Chin. Chem. Lett.* **1992**, *3*, 663–664; e) S. Takenaka, Y. Masuda, M. Iwano, H. Morita, S. Kusabayashi, H. Sigiura, T. Ikemoto, *Mol. Cryst. Liq. Cryst.* **1989**, *168*, 111–124; f) G. Lattermann, *Liq. Cryst.* **1987**, *2*, 723–728; g) S. Takenaka, K. Nishimura, S. Kusabayashi, *Mol. Cryst. Liq. Cryst.* **1984**, *111*, 227–236.

[18] a) M. Lehmann, R. I. Gearba, M. H. J. Koch, D. Ivanov, *Chem. Mater.* **2004**, *16*, 374–376; b) M. Lehmann, R. I. Gearba, M. H. J. Koch, D. Ivanov, *Mol. Cryst. Liq. Cryst.* **2004**, *411*, 397–406.

[19] S. Gemming, M. Lehmann, G. Seifert, *Z. Metallkd.* **2005**, *96*, 988–997.

[20] H. Meier, E. Karpouk, M. Lehmann, D. Schollmeyer, V. Enkelmann, *Z. Naturforsch. B* **2003**, *58*, 775–781.

[21] M. Lehmann, M. Jahr, T. Rüffer, H. Lang, *Z. Naturforsch. B* **2007**, *62*, 988–994.

[22] R. J. Bushby, O. R. Lozman, *Curr. Opin. Colloid Interface Sci.* **2002**, *7*, 343–354.

[23] a) R. I. Gearba, D. V. Anokhin, A. I. Bondar, W. Bras, M. Jahr, M. Lehmann, D. A. Ivanov, *Adv. Mater.* **2007**, *19*, 815–820; b) D. A. Ivanov, R. I. Gearba, D. Anokhin, S. Magonov, M. Lehmann, *PMSE Prepr.* **2006**, *94*, 655–656; c) R. I. Gearba, A. Bondar, M. Lehmann, B. Goderis, W. Bras, M. H. J. Koch, D. A. Ivanov, *Adv. Mater.* **2005**, *17*, 671–676.

[24] F. L. Weitl, *J. Org. Chem.* **1976**, *41*, 2044–2045.

[25] M. Lehmann, M. Jahr, unpublished results.

[26] a) P. Oswald, P. Pieranski, *Smectic and Columnar Liquid Crystals*, Taylor and Francis, Boca Raton, **2006**; b) Y. Bouligand, *J. Physique* **1980**, *41*, 1307–1315; c) C. Destrade, P. Foucher, H. Gasparoux, Nguyen Huu Tinh, A. M. Levelut, J. Malthête, *Mol. Cryst. Liq. Cryst.* **1984**, *106*, 121–146.

[27] M. Delaye, R. Ribotta, G. Durand, *Phys. Lett. A* **1973**, *44*, 139–140.

[28] The pattern forming in the dark brushes of the pseudo-focal-conic texture was visible with normal illumination; however, for the digital camera used, the features only became discernible on the image

when the sensitivity was increased, thus some areas appear to be over-illuminated.
[29] Compounds **1c** and **1d** have been extruded from the low-temperature orthorhombic mesophases owing to the low stability in their hexagonal columnar phases.
[30] Undulations have been observed in lamellar phases, see: A. Yamaguchi, Y. Maeda, H. Yokoyama, A. Yoshizawa, *Chem. Mater.* **2006**, *18*, 5704–5710, and references therein; they have also been observed at transitions from lamellar to columnar phases, see: D. Guillon, *Struct. Bonding (Berlin)* **1999**, *95*, 41–82; from columnar to cubic phases, see: B. Donnio, B. Heinrich, T. Gulik-Krywicki, H. Delacroix, D. Guillon, D. W. Bruce, *Chem. Mater.* **1997**, *9*, 2951–2965; and in polyelectrolyte–ionic surfactant complexes, see: M. Antonietti, J. Conrad, *Angew. Chem.* **1994**, *106*, 1927–1929; *Angew. Chem. Int. Ed. Engl.* **1994**, *33*, 1869–1870; the phenomenon originates from the different volumes needed to pack alkyl chains and the core and is also called "frustration".
[31] a) R. Jenkens, R. L. Snyder *Introduction to X-ray Powder Diffractometry, Vol 138 in Chemical Analysis*, Wiley, New York, **1996**; b) P. Scheerer, *Nachr. Ges. Wiss. Göttingen, Math.-Phys. Kl.* **1918**, *2*, 96–100.
[32] I. Schnell, H. W. Spiess, *J. Magn. Reson.* **2001**, *151*, 153–227.
[33] M. Feike, D. E. Demco, R. Graf, J. Gottwald, S. Hafner, H. W. Spiess, *J. Magn. Reson. Ser. A* **1996**, *122*, 214–221.
[34] D. Sebastiani, *ChemPhysChem* **2006**, *7*, 164–175.
[35] Extensive quantum-chemical molecular-dynamics simulations at room temperature exhibit fluctuations for the central benzene ring, which comprise relative lateral shifts of up to 0.5 Å and relative tilt angles of up to 20° between adjacent monomers within the columns, see: S. Gemming, I. Popov, M. Lehmann, *Philos. Mag. Lett.* **2007**, *87*, 883–891.
[36] M. Marcos, R. Giménez, J.-L. Serrano, B. Donnio, B. Heinrich, D. Guillon, *Chem. Eur. J.* **2001**, *7*, 1006–1013.
[37] L. J. Yu, Ch.-Ch. Cho, *Mol. Cryst. Liq. Cryst.* **2004**, *411*, 313–318.
[38] B. Donnio, B. Heinrich, H. Allouchi, J. Kain, S. Diele, D. Guillon, D. W. Bruce, *J. Am. Chem. Soc.* **2004**, *126*, 15258–15268.
[39] Similar high values for the *c* parameter are obtained for stacks of bowl-shaped conformers.
[40] The experimental average distance of aromatic units is 4.4 Å. With respect to the inclination of molecules by 60°, the separation of the dimers would amount to 8.8 Å (4.4 Å/cos 60°). However, if 5.5 dimers (11 molecules) are in the unit cell, then the periodicity would be 5.5×8.8 Å $= 48.4$ Å, which is not in agreement with the experimentally observed distance of 34 Å. A separation of dimers by 6.2 Å explains the observed periodicity along the column perfectly. Coplanar molecules inclined by 60° with respect to the columnar axis would then be separated by 3.1 Å. Nevertheless, this distance increases by rotational displacement of the aromatic segments within the helix.
[41] Two *E*-shaped molecules cover less than 360° of a columnar area; an azimuthal angle ω of approximately 20 to 40° remains unoccupied. We assume that this space will be filled by the next mesogen in the column by rotational displacement about that angle ω. Because rotation by 180° is achieved after 5.5 molecules, the rotation angle is calculated to be $\omega = 180°/5.5 = 33°$.
[42] M. Elstner, Th. Frauenheim, E. Kaxiras, G. Seifert, S. Suhai, *Phys. Status Solidi B* **2000**, *217*, 357–376.
[43] L. Zhechkov, T. Heine, S. Patchkovskii, G. Seifert, H. A. Duarte, *J. Chem. Theory Comput.* **2005**, *1*, 841–847.
[44] S. Gemming, M. Schreiber, W. Thiel, Th. Heine, G. Seifert, H. de Abreu, H. Duarte, *J. Lumin.* **2004**, *108*, 143–147.
[45] T. C. Huang, H. Toraya, T. N. Blanton, J. Wu, *J. Appl. Crystallogr.* **1993**, *26*, 180–184.
[46] http://www.datasqueezesoftware.com/.
[47] 1,3,5-Trihydroxy-2,4,6-trideuteriobenzene was prepared by heating dry phloroglucinol in D_2O at reflux.

Received: June 17, 2007
Published online: February 25, 2008

